

Rapid report

Anaplerotic flux into the Calvin–Benson cycle: hydrogen isotope evidence for *in vivo* occurrence in C₃ metabolism

Author for correspondence:
Thomas Wieloch
Email: thomas.wieloch@umu.se

Thomas Wieloch¹ , Angela Augusti²  and Jürgen Schleucher¹ 

¹Department of Medical Biochemistry and Biophysics, Umeå University, Umeå 90187, Sweden; ²Research Institute on Terrestrial Ecosystems, National Research Council, Porano (TR) 05010, Italy

Received: 6 August 2021
Accepted: 22 December 2021

New Phytologist (2022) 234: 405–411
doi: 10.1111/nph.17957

Key words: Calvin–Benson cycle, flux estimation, glucose-6-phosphate shunt, hydrogen stable isotopes, nitrogen assimilation, oxidative pentose phosphate pathway, plant carbon metabolism, source–sink balance.

Summary

- As the central carbon uptake pathway in photosynthetic cells, the Calvin–Benson cycle is among the most important biochemical cycles for life on Earth. A carbon flux of anaplerotic origin (i.e. through the chloroplast-localized oxidative branch of the pentose phosphate pathway) into the Calvin–Benson cycle was proposed recently.
- Here, we measured intramolecular deuterium abundances in leaf starch of *Helianthus annuus* grown at varying ambient CO₂ concentrations, C_a. Additionally, we modelled deuterium fractionations expected for the anaplerotic pathway and compared modelled with measured fractionations.
- We report deuterium fractionation signals at H¹ and H² of starch glucose. Below a C_a change point, these signals increase with decreasing C_a consistent with modelled fractionations by anaplerotic flux. Under standard conditions (C_a = 450 ppm corresponding to intercellular CO₂ concentrations, C_i, of 328 ppm), we estimate negligible anaplerotic flux. At C_a = 180 ppm (C_i = 140 ppm), more than 10% of the glucose-6-phosphate entering the starch biosynthesis pathway is diverted into the anaplerotic pathway.
- In conclusion, we report evidence consistent with anaplerotic carbon flux into the Calvin–Benson cycle *in vivo*. We propose the flux may help to: maintain high levels of ribulose 1,5-bisphosphate under source-limited growth conditions to facilitate photorespiratory nitrogen assimilation required to build-up source strength; and counteract oxidative stress.

Introduction

In photosynthetic cells, carbon is taken up primarily by the Calvin–Benson cycle (CBC). Thus, the CBC is among the most important biochemical cycles for life on Earth. Sharkey & Weise (2016) proposed the CBC may be anaplerotically refilled by carbon injection from the oxidative branch of the chloroplast-localized pentose phosphate pathway (namely, glucose-6-phosphate (G6P) shunt, orange pathway in Fig. 1). This pathway liberates CO₂ from metabolism and anaplerotically recovered energy (nicotinamide adenine dinucleotide phosphate, NADPH) is insufficient for quantitative refixation. Should this flux occur *in vivo*, it would therefore affect plant carbon and energy balances, plant performance, ecosystem productivity, and biosphere–atmosphere CO₂ exchange. This includes the CO₂ fertilization effect which has been

identified as a major unknown in our current Earth system understanding (IPCC, 2013) as well as future atmospheric CO₂ concentrations and crop yields (cf. Long *et al.*, 2006).

Anaplerotic flux is believed to be controlled at phosphoglucose isomerase (PGI, EC 5.3.1.9; green in Fig. 1) which catalyses interconversions of fructose 6-phosphate (F6P) and G6P (Sharkey & Weise, 2016). In the light, the reaction is strongly displaced from equilibrium on the side of F6P keeping chloroplastic G6P concentrations low (Dietz, 1985; Gerhardt *et al.*, 1987; Kruckeberg *et al.*, 1989; Schleucher *et al.*, 1999) proposedly to restrict the anaplerotic flux (Sharkey & Weise, 2016). With decreasing PGI inhibitor concentrations (3-phosphoglycerate, and especially erythrose 4-phosphate), the PGI reaction shifts towards equilibrium (Dietz, 1985; Backhausen *et al.*, 1997). Concomitantly increasing G6P concentrations (Dietz, 1985) may cause anaplerotic flux

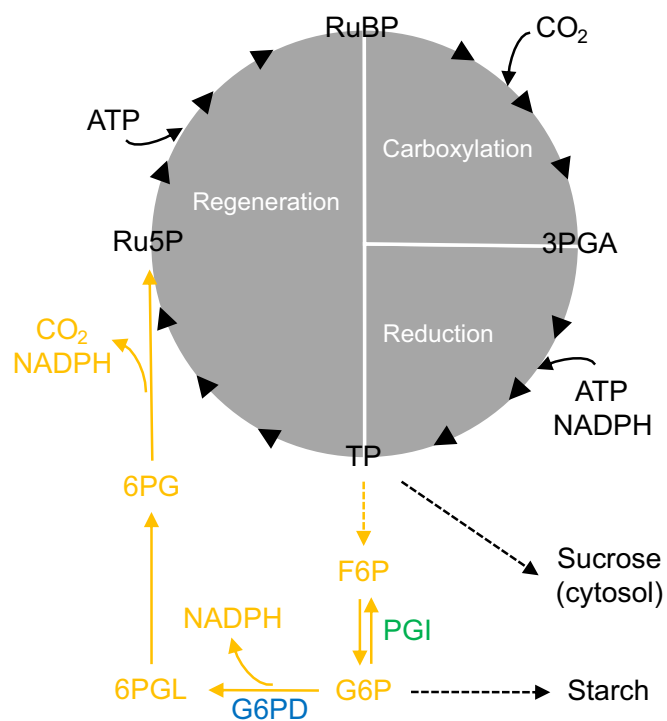


Fig. 1 Oxidative branch of the chloroplast-localized pentose phosphate pathway (in orange) carrying anaplerotic carbon flux into the Calvin–Benson cycle (in grey). Blue and green, enzyme reactions that may introduce deuterium fractionation signals at glucose H¹ and H², respectively. Dashed arrows, intermediate reactions not shown. Enzymes, G6PD, glucose-6-phosphate dehydrogenase; PGI, phosphoglucose isomerase. Metabolites: 3PGA, 3-phosphoglycerate; 6PG, 6-phosphogluconate; 6PGL, 6-phosphogluconolactone; ATP, adenosine triphosphate; F6P, fructose 6-phosphate; G6P, glucose 6-phosphate; NADPH, nicotinamide adenine dinucleotide phosphate; Ru5P, ribulose 5-phosphate; RuBP, ribulose 1,5-bisphosphate; TP, triose phosphates (glyceraldehyde 3-phosphate, dihydroxyacetone phosphate). Modified figure from Wieloch *et al.* (2022).

increases by the following mechanism (Sharkey & Weise, 2016). In the light, the first enzyme of the pentose phosphate pathway, glucose-6-phosphate dehydrogenase (G6PD, EC 1.1.1.49; blue in Fig. 1), is inhibited by redox regulation via thioredoxin (Née *et al.*, 2009). However, inhibition can be reversed allosterically by increasing G6P concentrations (Cossar *et al.*, 1984; Preiser *et al.*, 2019).

While anaplerotic flux into the CBC seems biochemically feasible, so far, only three studies have reported flux-level evidence. First, Wieloch *et al.* (2018) analysed intramolecular ¹³C/¹²C ratios in glucose extracted from an annually resolved *Pinus nigra* tree-ring series (1961–1995). They reported ¹³C fractionation signals (i.e. systematic ¹³C/¹²C variation) at glucose C-1 and C-2. These signals respond to drought proposedly due to changes in anaplerotic flux by the following mechanism (Wieloch *et al.*, 2018). As isohydric species, *P. nigra* responds to drought by stomatal closure which impedes CO₂ uptake causing low intercellular CO₂ concentrations, C_i (Sade *et al.*, 2012). With decreasing C_i, PGI inhibitor concentrations reportedly decrease, and the chloroplastic PGI reaction shifts towards equilibrium (Badger *et al.*, 1984; Dietz & Heber, 1984; Dietz, 1985). Concomitantly increasing G6P

concentrations can be expected to cause increasing G6PD activity and anaplerotic flux (see last paragraph). Based on reported ¹³C isotope effects (Gilbert *et al.*, 2012), Wieloch *et al.* (2018) predicted ¹³C/¹²C increases at C-1 and C-2 at a ratio of 2.25 in response to shifts of the PGI reaction towards equilibrium and found a ratio of 2.74 (+1.35SE, –0.60SE) confirming their prediction. Interestingly, the reported ratio is somewhat higher than the predicted ratio yet not significantly. Still, the offset may be explained by the ¹³C effect of G6PD ($\alpha = 1.0165$; Hermes *et al.*, 1982) which can be expected to cause an additional ¹³C/¹²C increase at C-1 as anaplerotic flux increases.

Second, Wieloch *et al.* (2022) also analysed intramolecular deuterium (D) abundances across the *P. nigra* tree-ring series. They reported two closely related D fractionation signals at glucose H¹ and H² which respond to drought and atmospheric CO₂ concentrations. Interestingly, the response requires the crossing of a change point. Wieloch *et al.* (2022) hypothesize that shifts of the chloroplastic PGI reaction towards equilibrium contribute to the signal at H² while chloroplastic G6PD contributes to the H¹ signal as anaplerotic flux changes.

Third, Xu *et al.* (2021) analysed ¹³C enrichment patterns of central metabolites in *Camelina sativa* leaves by ¹³C isotopically nonstationary metabolic flux analysis. They reported estimates for anaplerotic flux (4.6 $\mu\text{mol CO}_2 \text{ g}^{-1}$ fresh weight (FW) h⁻¹, c. 3% of Rubisco carboxylation) and day respiration (5.2 $\mu\text{mol CO}_2 \text{ g}^{-1}$ FW h⁻¹). However, these estimates come from a physiologically unrealistic model and could not be confirmed by independent methods (Wieloch, 2021). In summary, Xu *et al.* (2021) reported evidence for anaplerotic flux under normal growth conditions while Wieloch *et al.* (2018, 2022) reported evidence for stress-induced upregulation.

To explain the ¹³C and D fractionation signals observed in tree-ring glucose of the gymnosperm *P. nigra*, Wieloch *et al.* (2022) proposed the following hypotheses. First, anaplerotic flux into the CBC is associated with D fractionation signals at H¹ and H² of chloroplastic G6P and its derivatives including leaf starch. Second, anaplerotic flux and associated D signals increase with decreasing C_i. Third, increases occur below a C_i change point. In addition, these authors discussed whether anaplerotic flux is a general feature of C₃ metabolism. To test these hypotheses in combination, we analysed intramolecular D abundances in leaf starch of the angiosperm *Helianthus annuus* synthesized at varying C_i. In addition, we discuss the anaplerotic flux in the context of plant physiology and climate change.

Materials and Methods

Samples

We used samples of the C₃ plant *H. annuus* L. cv Zebulon from a previous study (Ehlers *et al.*, 2015). These plants were raised in 1.4 l pots in a glasshouse at an ambient CO₂ concentration of C_a \approx 450 ppm and a light intensity of 300–400 $\mu\text{mol photons m}^{-2} \text{ s}^{-1}$ (16 h photoperiod). They were watered daily, fertilized twice a week with Rika-S (Weibulls, Hammenhög, Sweden) and transferred to a growth chamber in groups of eight after 7–8 wk.

Growth chamber temperature and relative humidity was set to 22°C : 18°C and 60% : 70% (day : night), respectively. On the first day after transfer, the plants were kept in darkness at $C_a = 450$ ppm to drain the starch reserves. During the following 2 days, the plant groups were grown at a C_a of either 180, 280, 450, 700, or 1500 ppm (300–400 $\mu\text{mol photons m}^{-2} \text{s}^{-1}$, 16 h photoperiod). On the second day, gas exchange measurements were performed (Supporting Information Notes S1), and leaves were harvested and stored at -20°C until starch extraction described in Ehlers *et al.* (2015). Reported C_i values were estimated as described in the Notes S2.

Determination and expression of intramolecular deuterium abundances

Intramolecular D abundances in starch glucose were measured following published procedures (Betson *et al.*, 2006; Ehlers *et al.*, 2015). Proton nuclear magnetic resonance ($^1\text{H-NMR}$) spectroscopy was used to ensure sample purity of the glucose derivative used for quantification (3,6-anhydro-1,2-*O*-isopropylidene- α -D-glucofuranose) of $\geq 99.5\%$. We recorded quantitative D NMR spectra on a DRX600 spectrometer with 5-mm broadband observe probe and ^{19}F lock (Bruker BioSpin GmbH, Rheinstetten, Germany). Relative intramolecular D abundances were determined by signal deconvolution using Lorentzian line shape fits in TOPSPIN 3.1 (Bruker BioSpin GmbH). To screen for intramolecular fractionations, we expressed the data as deviations from the molecular average as

$$\Delta D_i = \frac{D_i}{\sum D_i/7} - 1 \quad \text{Eqn 1}$$

D_i denotes relative D abundances at specific glucose hydrogen positions. In this notation, whole-molecule effects are not expressed. However, the size of any intramolecular fractionation effect is attenuated by its contribution to the denominator. To obtain estimates of effect sizes, we used as reference the average D abundance of the methyl-group hydrogens of the glucose derivative (introduced during derivatization from a common batch of acetone) as

$$\delta D_i = \frac{D_i}{\sum D_{\text{ME}}/6} - 1 \quad \text{Eqn 2}$$

D_{ME} denotes relative D abundances of the methyl-group hydrogens.

Results

Deuterium enrichments at glucose H^1 , and H^2

Here, we analysed intramolecular D abundances in *H. annuus* leaf starch synthesized at different levels of C_a (180, 280, 450, 700, and 1500 ppm). We found intramolecular fractionations at H^1 and H^2 (Fig. 2). With decreasing C_a from 450 to 180 ppm (C_i from 328 to 140 ppm), δD increases at H^1 (210‰), and H^2 (311‰, Fig. 3).

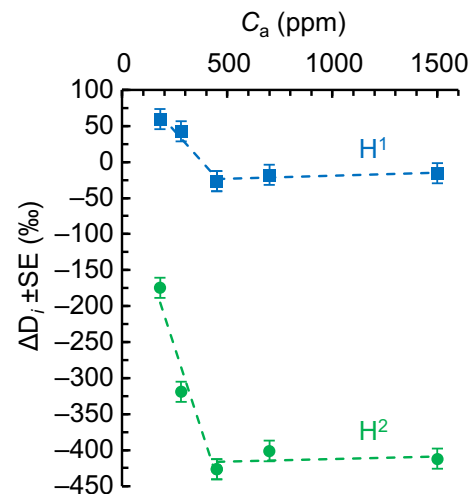


Fig. 2 Relative deuterium (D) abundance at H^1 (blue squares), and H^2 (green circles) of *Helianthus annuus* leaf starch. Plants were grown in chambers at ambient CO_2 concentration (C_a) = 450 ppm. After a day in darkness to drain starch reserves, plants were grown at different levels of C_a (180, 280, 450, 700, and 1500 ppm) corresponding to different levels of intercellular CO_2 concentration (C_i) (140, 206, 328, 531, and 1365 ppm) for 2 d. Data expressed in terms of the molecular average as $\Delta D_i = D_i/(\sum D_i/7) - 1$, where D_i denotes relative D abundances at specific glucose hydrogen positions ($\pm \text{SE} = 14.1\%$). Figure shows discrete data. Dashed lines added to guide the eye.

Note that actual offsets may be somewhat larger than apparent offsets (Notes S3). Above $C_a = 450$ ppm ($C_i \approx 328$ ppm), these relationships break, i.e. they exhibit a change point at $C_a \approx 450$ ppm. In general, intramolecular fractionations are caused by metabolic processes (see next paragraphs).

Photorespiratory deuterium fractionations occur at glucose H^1 , and $\text{H}^{6\text{S}}$

With decreasing C_a from 450 to 180 ppm (C_i from 328 to 140 ppm), δD increases at H^1 (210‰), and $\text{H}^{6\text{S}}$ (127‰) but not $\text{H}^{6\text{R}}$ (Fig. 3). Changing photorespiration-to-photosynthesis ratios reportedly has equal effects on both the $\text{H}^{6\text{R}}/\text{H}^1$ and $\text{H}^{6\text{R}}/\text{H}^{6\text{S}}$ D abundance ratios (Schleucher, 1998). This was attributed to changes at $\text{H}^{6\text{R}}$ (Schleucher, 1998). However, $\delta D_{6\text{R}}$ is invariable between 450 and 180 ppm (Fig. 3b). Thus, photorespiratory fractionation likely occurs at glucose H^1 and $\text{H}^{6\text{S}}$ but not $\text{H}^{6\text{R}}$.

Metabolic origin of the deuterium enrichment at glucose H^1

Starch biosynthesis from photosynthetic glyceraldehyde 3-phosphate (GAP) proceeds via a multi-step enzymatic pathway (Fig. 4). In the first step, triosephosphate isomerase converts GAP (glucose C-4 to C-6) to dihydroxyacetone phosphate (DHAP) (glucose C-1 to C-3). Thereby, the GAP hydrogen corresponding to glucose $\text{H}^{6\text{S}}$ becomes the DHAP hydrogen corresponding to glucose H^1 . These hydrogens are neither modified by the triosephosphate isomerase reaction, nor by any subsequent reaction leading to starch. Hence, starch glucose $\text{H}^{6\text{S}}$ and H^1 can be expected to have equal D abundances. Evidently, this situation occurs at

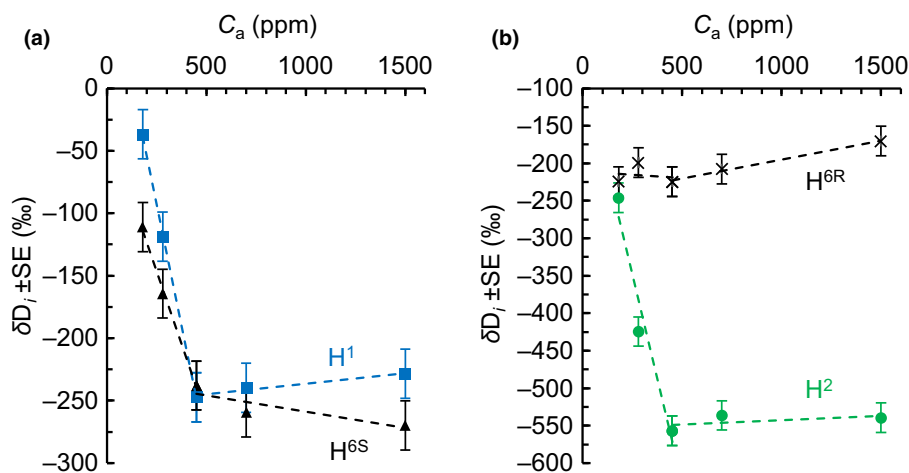


Fig. 3 (a, b) Relative deuterium (D) abundance at H^1 (blue squares), H^{6S} (black triangles), H^2 (green circles), and H^{6R} (black crosses) of *Helianthus annuus* leaf starch. Plants were grown in chambers at ambient CO_2 concentration (C_a) = 450 ppm. After a day in darkness to drain starch reserves, plants were grown at different levels of C_a (180, 280, 450, 700, and 1500 ppm) corresponding to different levels of intercellular CO_2 concentration (C_i) (140, 206, 328, 531, and 1365 ppm) for 2 d. Data expressed as $\delta D_i = D_i / (\Sigma D_{ME} / 6) - 1$, with D_i and D_{ME} denoting relative D abundances at specific glucose hydrogen positions and the methyl-group hydrogens of the glucose derivative used for measurements, respectively ($\pm SE = 19.7\%$). Figure shows discrete data. Dashed lines added to guide the eye.

$C_a = 450$ ppm (Fig. 3a). Thus, there is no evidence for anaplerotic fractionation and flux at $C_a = 450$ ppm (under standard conditions) suggesting that G6PD is efficiently inhibited by thioredoxin despite the relatively low light intensity.

Equal D enrichments at H^1 and H^{6S} can be attributed to photorespiratory fractionation (see previous paragraph). However, at $C_a = 180$ ppm, H^1 is 74‰ more enriched than H^{6S} (Fig. 3a; $\delta D_1 = -37\%$, $\delta D_{6S} = -111\%$). This enrichment can be expected to be introduced beyond DHAP synthesis by a high-flux carrying pathway branching off from the starch biosynthesis pathway. To our knowledge, there are only two possible candidates, the well-established CBC-regeneration pathway and the proposed anaplerotic pathway (Fig. 4). The former pathway starts with the conversion of F6P and GAP to erythrose 4-phosphate and xylulose 5-phosphate by transketolase. The hydrogen corresponding to starch glucose H^1 is not modified by the transketolase reaction. By contrast, the anaplerotic pathway starts with the irreversible G6PD-catalysed conversion of G6P to 6-phosphogluconolactone which deprotonates the G6P hydrogen corresponding to starch glucose H^1 . This reaction reportedly has a D isotope effect *in vitro* ($\alpha_D = k_H/k_D = 2.97$) (Hermes *et al.*, 1982). Thus, G6PD is a plausible candidate for D fractionation at H^1 .

Consistent with our observations, fractionation modelling shows that increasing anaplerotic flux, f , causes D increases at H^1 of remaining G6P, δD_{G6P} (Fig. 5; Notes S4). A 74‰ increase as observed in starch (Fig. 3a) indicates that *c.* 10% of the G6P entering the starch biosynthesis pathway is diverted into the anaplerotic pathway. However, G6P can be converted back to F6P by PGI and enter the CBC via transketolase (Fig. 4). This flux will be low under low chloroplastic G6P concentrations (i.e. under standard growth conditions) yet increase as the PGI reaction shifts towards equilibrium (with shifts towards low C_a , see the ‘Introduction’ section). It can be expected to fractionally remove the G6PD-fractionation signal from the starch biosynthesis

pathway. Thus, at $C_a = 180$ ppm, more than 10% of the G6P entering the starch biosynthesis pathway may be diverted into the anaplerotic pathway (to obtain a 74‰ increase at H^1).

Metabolic origin of the deuterium enrichment at glucose H^2

At the level of chloroplastic triose phosphates, the precursors of starch glucose H^2 correspond to the precursors of starch glucose H^{6R} (Fig. 4). In the biosynthetic pathway from triose phosphate to starch, the former is subject to modification by PGI while the latter is not modified. Therefore, we assume the D abundance at H^{6R} is not modified during starch biosynthesis and can be used as reference for H^2 .

Under standard conditions ($C_a = 450$ ppm), starch glucose H^2 is 311‰ depleted compared to low C_a conditions (= 180 ppm) and 332‰ depleted compared to H^{6R} (Fig. 3b). This is consistent with reported glucose H^2 depletions in leaf starch compared to sucrose (*Phaseolus vulgaris*, 333‰; *Spinacia oleracea*, 500‰) which were explained by different *modus operandi* of chloroplastic and cytosolic PGI (Schleucher *et al.*, 1999). Reportedly, the chloroplastic PGI reaction is strongly displaced from equilibrium on the side of F6P (Dietz, 1985; Gerhardt *et al.*, 1987; Leidreiter *et al.*, 1995; Schleucher *et al.*, 1999) while the cytosolic reaction is either somewhat displaced from equilibrium (Leidreiter *et al.*, 1995; Schleucher *et al.*, 1999) or at equilibrium (Gerhardt *et al.*, 1987). Thus, in chloroplasts under standard conditions, the kinetic isotope effect of PGI is manifested. This effect can cause D depletions of up to *c.* 550‰ (Notes S5; hydrogen exchange with the medium not considered).

At low C_a (= 180 ppm), starch glucose H^2 is merely 21.5‰ depleted compared to H^{6R} (Fig. 3b). This is consistent with a shift of the PGI reaction from kinetic to equilibrium conditions and thus upregulated anaplerotic flux (see the ‘Introduction’ section). Theoretically, equilibrium isotope fractionation by PGI causes a D

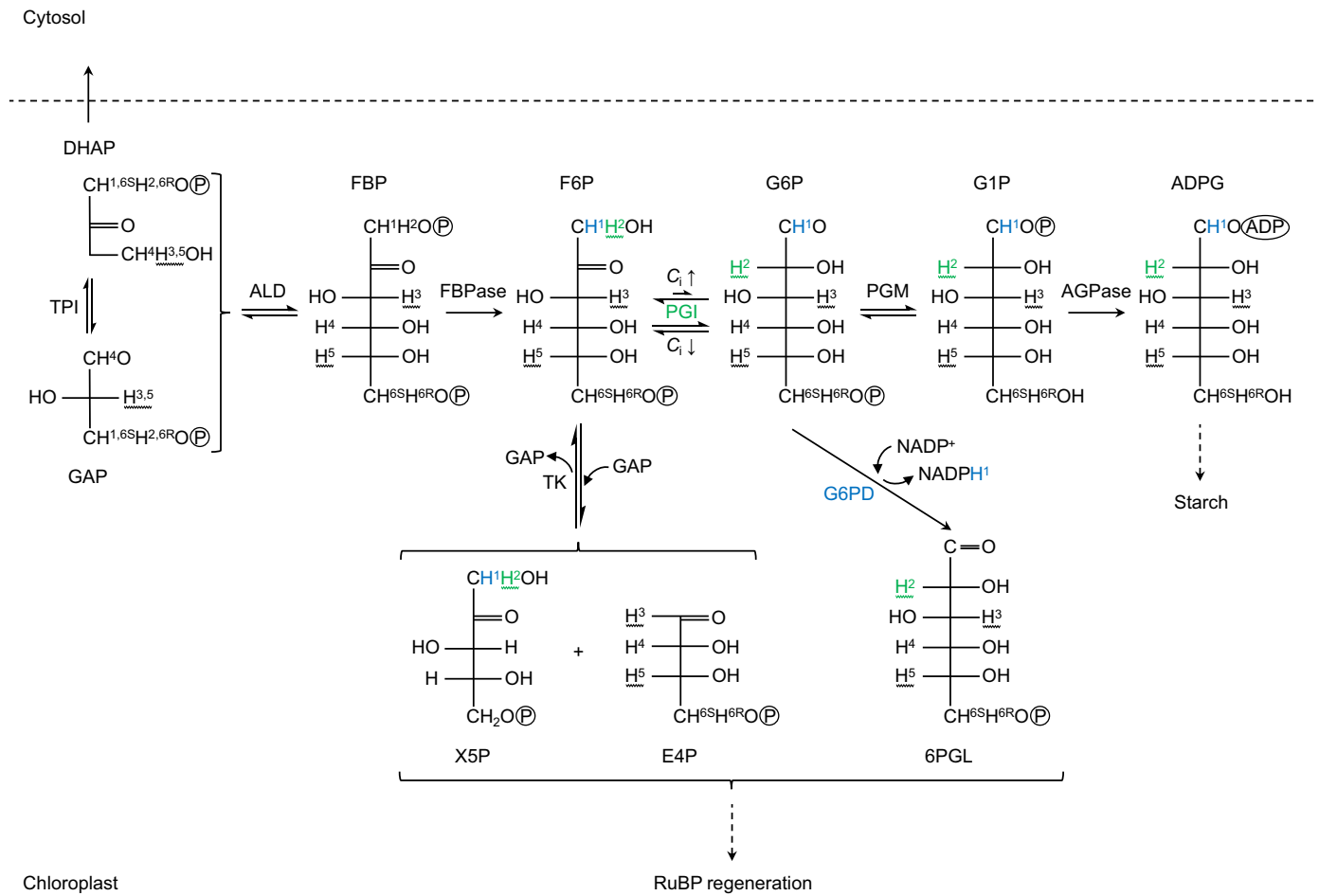


Fig. 4 Hydrogen metabolism associated with starch biosynthesis. Hydrogens named according to their location(s) in starch glucose (indirect precursors not designated, see X5P). Green and blue hydrogens may be affected by isotope fractionation at PGI and G6PD, respectively. Wavy lines, hydrogen from water is fractionally introduced during the TPI and PGI reaction. Under standard C_i conditions ($C_i \uparrow$), the chloroplastic PGI reaction is strongly displaced from equilibrium on the side of F6P. Under low C_i conditions ($C_i \downarrow$), the chloroplastic PGI reaction is closer to or at equilibrium. Dashed arrows, Intermediate reactions not shown. Abbreviations: 6PGL, 6-phosphogluconolactone; ADPG, ADP-glucose; AGPase, glucose-1-phosphate adenyltransferase; ALD, fructose-1,6-bisphosphate aldolase; C_i , intercellular CO_2 concentration; DHAP, dihydroxyacetone phosphate; E4P, erythrose 4-phosphate; F6P, fructose 6-phosphate; FBP, fructose 1,6-bisphosphate; FBPase, fructose 1,6-bisphosphatase; G1P, glucose 1-phosphate; G6P, glucose 6-phosphate; G6PD, glucose-6-phosphate dehydrogenase; GAP, glyceraldehyde 3-phosphate; PGI, phosphoglucose isomerase; PGM, phosphoglucomutase; RuBP, ribulose 1,5-bisphosphate; TK, transketolase; TPI, triose-phosphate isomerase; X5P, xylulose 5-phosphate.

depletion of $\approx 99\%$ when fractionation related to hydrogen exchange with the medium is not considered (Notes S5). However, the offset between theoretical and observed values (*c.* 77.5%) indicates that hydrogen exchange with the medium affects isotope fractionation by PGI.

Discussion

Consistent with isotope theory related to anaplerotic carbon flux into the CBC (see the ‘Introduction’ section; Wieloch *et al.*, 2022), we found D fractionation signals at H^1 and H^2 of leaf starch which increase with decreasing C_a (and C_i) below a response change point (Figs 2, 3). Under standard conditions ($C_a = 450$ ppm, $C_i = 328$ ppm), we estimate negligible anaplerotic flux. This is in contrast to findings by Xu *et al.* (2021). At $C_a = 180$ ppm ($C_i = 140$ ppm), we estimate that more than 10% of the G6P entering the starch biosynthesis pathway is diverted into the anaplerotic pathway.

Previously, we reported evidence for anaplerotic flux in *P. nigra*, a gymnosperm (Wieloch *et al.*, 2018, 2022). Here, we report evidence for this flux in the angiosperm *H. annuus* (Figs 2, 3). Thus, anaplerotic flux into the CBC may be a general component of C_3 metabolism. Lastly, our data suggest photorespiratory fractionation affects the D abundance at glucose H^1 and H^{6S} but not H^{6R} .

Anaplerotic flux into the Calvin–Benson cycle: a leaf-level response to source–sink imbalances?

In *H. annuus*, anaplerotic flux was upregulated under apparent steady-state conditions at low C_a concentrations (Figs 2, 3). Similarly, large anaplerotic isotope fractionations in *P. nigra* tree rings (formed over the course of several months) suggest that the anaplerotic flux can persist over long periods (Wieloch *et al.*, 2018, 2022).

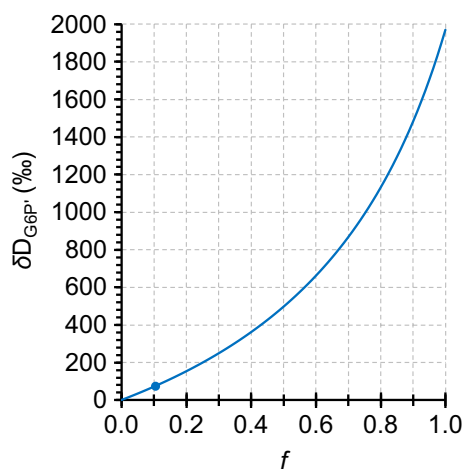


Fig. 5 Modelled deuterium (D) fractionation by glucose-6-phosphate dehydrogenase (G6PD) at H¹ of glucose 6-phosphate (G6P), δD_{G6P} . Modelling assumed an open system at steady state. Incoming G6P has two fates, starch biosynthesis or anaplerotic reinjection into the Calvin–Benson cycle via G6PD (Fig. 4). Commitment of G6P to the anaplerotic pathway vs starch biosynthesis, f , is given on the abscissa (e.g. $f = 1$: all G6P enters the anaplerotic pathway, $f = 0$: all G6P enters starch biosynthesis). Blue dot, $f = 0.1044$, $\delta D_{G6P} = 74.41\%$. G6PD has an *in vitro* kinetic isotope effect of $\alpha_D = 2.97$ (Hermes *et al.*, 1982). G6P entering the system was assumed to have the same D : H ratio as Vienna Standard Mean Ocean Water ($R_{VSMOW} = 155.76 \times 10^{-6}$) (Hagemann *et al.*, 1970). Data expressed in terms of R_{VSMOW} .

Helianthus annuus was raised at $C_a = 450$ ppm over 7–8 wk. After a day in darkness, the plants were subjected to different C_a treatments for 2 d. We found evidence for anaplerotic flux at $C_a < 450$ ppm (Figs 2, 3). This may be explained by a shift from the plants' previously established source–sink balance at $C_a = 450$ ppm to source-limited conditions at $C_a < 450$ ppm (where sink demands exceed the source strength). A concomitant downstream pull of carbohydrates may have caused excess export of triose phosphates from chloroplasts to the cytosol and shortage of chloroplastic triose phosphates for regeneration of ribulose 1,5-bisphosphate (RuBP) (Fig. 4). To maintain the photosynthetic/photorespiratory capacity at the level of RuBP, anaplerotic flux may then have been upregulated by mechanisms described earlier (see the 'Introduction' section). Thus, we propose upregulation of the anaplerotic flux is a leaf-level response to source-limited growth conditions. It may be triggered by all environmental parameters that can cause source limitations such as low C_a , low C_i , and drought (as in *P. nigra*) (Wieloch *et al.*, 2018, 2022). This may have implications for gas exchange studies aiming to investigate actual steady-state conditions. To preclude errors due to anaplerotic CO₂ liberation associated with disturbed source–sink balances, plants should be raised under the same conditions they are analysed.

Anaplerotic flux into the Calvin–Benson cycle: potential benefits for plant functioning and growth

Like photorespiration, anaplerotic flux has a negative carbon balance (Fig. 1) and seems, therefore, detrimental for plant functioning and growth but we propose two potential benefits.

First, by maintaining RuBP levels, anaplerotic flux maintains photorespiration (both fluxes increase with decreasing C_a and C_i).

Reportedly, photorespiration is positively correlated with *de novo* nitrate assimilation into protein (Bloom, 2015). Thus, anaplerotic flux may help to increase photosynthetic capacity at the enzyme level, and it seems plausible that plants would try to increase this capacity under source-limited conditions. Additionally, increased nitrogen assimilation may support the biosynthesis of nitrogen-containing compounds used for maintenance and repair processes. Overall, it seems plausible that metabolism would shift towards nitrogen assimilation when carbon metabolism is substrate limited.

Second, optimal plant functioning requires a balance between energy supply and consumption (Huner *et al.*, 1996). Upregulation of the anaplerotic flux occurs at low C_i (Figs 2, 3) which can cause energy imbalances in chloroplasts (Huner *et al.*, 1996; Wilhelm & Selmar, 2011; Vanlerberghe *et al.*, 2015). This involves decreased consumption of adenosine triphosphate (ATP) and NADPH by the CBC but constant electron input by light-harvesting complexes. The resulting lack of electron acceptors (NADP⁺ and adenosine diphosphate (ADP)) leads to the generation of reactive oxygen species (Vanlerberghe *et al.*, 2015). Futile carbon cycling involving CO₂ liberation by the anaplerotic flux and refixation by Rubisco has a negative NADPH and especially ATP balance (Fig. 1). Thus, anaplerotic flux may help to dissipate excess energy and counteract oxidative stress and photoinhibition at low C_i .

In *P. nigra*, upregulation of the anaplerotic pathway was reportedly associated with below-average yet not exceptionally low growth (Wieloch *et al.*, 2022). This is surprising since anaplerotic flux increases with decreasing C_i and liberates CO₂ (Figs 1–3). Principally, inputs of storage carbohydrates from previous years may have rescued growth rates but such inputs were shown to be negligible (Wieloch *et al.*, 2018). By contrast, physiological benefits proposed earlier may have contributed to maintaining growth rates.

Anaplerotic flux into the Calvin–Benson cycle and climate change




In *P. nigra*, anaplerotic flux reportedly correlates positively with drought and negatively with C_a (Wieloch *et al.*, 2018, 2022). This is consistent with findings reported here. The Intergovernmental Panel on Climate Change (IPCC) predicts a higher frequency of drought events in already dry regions towards the end of the 21st century (RCP8.5) (IPCC, 2013). Simultaneously, C_a will increase globally. Therefore, it is unclear whether photosynthesis involving an upregulated anaplerotic flux will become more prevalent.

Despite potentially significant impacts on carbon, nitrogen, and energy metabolism, the anaplerotic pathway is currently neither well understood nor considered in models of photosynthesis, biosphere–atmosphere CO₂ exchange, and plant growth. Stable isotope tools utilized here may enable comprehensive flux analyses across spatiotemporal scales.

Author contributions

TW conceived the study and led the research. AA and JS prepared the samples and acquired the data. TW analysed and interpreted the data. TW wrote the article with input from AA and JS.

ORCID

Angela Augusti  <https://orcid.org/0000-0002-9591-693X>
Jürgen Schleucher  <https://orcid.org/0000-0002-4815-3466>
Thomas Wieloch  <https://orcid.org/0000-0001-9162-2291>

Data availability

The data that support the findings of this study are available from the corresponding author upon reasonable request.

References

- Backhausen JE, Jöstingmeyer P, Scheibe R. 1997. Competitive inhibition of spinach leaf phosphoglucose isomerase isoenzymes by erythrose 4-phosphate. *Plant Science* 130: 121–131.
- Badger MR, Sharkey TD, von Caemmerer S. 1984. The relationship between steady-state gas exchange of bean leaves and the levels of carbon-reduction-cycle intermediates. *Planta* 160: 305–313.
- Batson TR, Augusti A, Schleucher J. 2006. Quantification of deuterium isotopomers of tree-ring cellulose using nuclear magnetic resonance. *Analytical Chemistry* 78: 8406–8411.
- Bloom AJ. 2015. Photorespiration and nitrate assimilation: a major intersection between plant carbon and nitrogen. *Photosynthesis Research* 123: 117–128.
- Cossar JD, Rowell P, Stewart WDP. 1984. Thioredoxin as a modulator of glucose-6-phosphate dehydrogenase in a N₂-fixing cyanobacterium. *Microbiology* 130: 991–998.
- Dietz K-J. 1985. A possible rate-limiting function of chloroplast hexosemonophosphate isomerase in starch synthesis of leaves. *Biochimica et Biophysica Acta* 839: 240–248.
- Dietz K-J, Heber U. 1984. Rate-limiting factors in leaf photosynthesis. I. Carbon fluxes in the Calvin cycle. *Biochimica et Biophysica Acta* 767: 432–443.
- Ehlers I, Augusti A, Batson TR, Nilsson MB, Marshall JD, Schleucher J. 2015. Detecting long-term metabolic shifts using isotopomers: CO₂-driven suppression of photorespiration in C₃ plants over the 20th century. *Proceedings of the National Academy of Sciences, USA* 112: 15585–15590.
- Gerhardt R, Stitt M, Heldt HW. 1987. Subcellular metabolite levels in spinach leaves: regulation of sucrose synthesis during diurnal alterations in photosynthetic partitioning. *Plant Physiology* 83: 399–407.
- Gilbert A, Robins RJ, Remaud GS, Tcherkez G. 2012. Intramolecular ¹³C pattern in hexoses from autotrophic and heterotrophic C₃ plant tissues. *Proceedings of the National Academy of Sciences, USA* 109: 18204–18209.
- Hagemann R, Nief G, Roth E. 1970. Absolute isotopic scale for deuterium analysis of natural waters. Absolute D/H ratio for SMOW. *Tellus* 22: 712–715.
- Hermes JD, Roeske CA, O'Leary MH, Cleland WW. 1982. Use of multiple isotope effects to determine enzyme mechanisms and intrinsic isotope effects. Malic enzyme and glucose 6-phosphate dehydrogenase. *Biochemistry* 21: 5106–5114.
- Huner NPA, Maxwell DP, Gray GR, Savitch LV, Krol M, Ivanov AG, Falk S. 1996. Sensing environmental temperature change through imbalances between energy supply and energy consumption: redox state of photosystem II. *Physiologia Plantarum* 98: 358–364.
- IPCC. 2013. Climate change 2013: the physical science basis. In: Stocker TF, Qin D, Plattner G-K, Tignor M, Allen SK, Boschung J, Nauels A, Xia Y, Bex V, eds. *Contribution of Working Group I to the Fifth Assessment Report of the Intergovernmental Panel on Climate Change*. Cambridge, UK and New York, NY, USA: Cambridge University Press.
- Kruckeberg AL, Neuhaus HE, Feil R, Gottlieb LD, Stitt M. 1989. Decreased-activity mutants of phosphoglucose isomerase in the cytosol and chloroplast of *Clarkia xantiana*. *Biochemical Journal* 261: 457–467.
- Leidreiter K, Kruse A, Heineke D, Robinson DG, Heldt H-W. 1995. Subcellular volumes and metabolite concentrations in potato (*Solanum tuberosum* cv. Désirée) leaves. *Botanica Acta* 108: 439–444.
- Long SP, Ainsworth EA, Leakey ADB, Nösberger J, Ort DR. 2006. Food for thought: lower-than-expected crop yield stimulation with rising CO₂ concentrations. *Science* 312: 1918–1921.
- Née G, Zaffagnini M, Trost P, Issakidis-Bourguet E. 2009. Redox regulation of chloroplastic glucose-6-phosphate dehydrogenase: a new role for f-type thioredoxin. *FEBS Letters* 583: 2827–2832.
- Preiser AL, Fisher N, Banerjee A, Sharkey TD. 2019. Plastidic glucose-6-phosphate dehydrogenases are regulated to maintain activity in the light. *Biochemical Journal* 476: 1539–1551.
- Sade N, Gebremedhin A, Moshelion M. 2012. Risk-taking plants: anisohydric behavior as a stress-resistance trait. *Plant Signaling & Behavior* 7: 767–770.
- Schleucher J. 1998. Intramolecular deuterium distributions and plant growth conditions. In: Griffiths H, ed. *Stable isotopes – integration of biological, ecological and geochemical processes*. Oxford, UK: Bios Scientific Publishers, 63–73.
- Schleucher J, Vanderveer P, Markley JL, Sharkey TD. 1999. Intramolecular deuterium distributions reveal disequilibrium of chloroplast phosphoglucose isomerase. *Plant, Cell & Environment* 22: 525–533.
- Sharkey TD, Weise SE. 2016. The glucose 6-phosphate shunt around the Calvin–Benson cycle. *Journal of Experimental Botany* 67: 4067–4077.
- Vanlerberghe GC, Wang J, Cvetkovska M, Dahal K. 2015. Modes of electron transport chain function during stress: does alternative oxidase respiration aid in balancing cellular energy metabolism during drought stress and recovery? In: Gupta KJ, Mur LAJ, Neelwarne B, eds. *Alternative respiratory pathways in higher plants*. Oxford, UK: John Wiley & Sons, 157–183.
- Wieloch T. 2021. The next phase in the development of ¹³C isotopically nonstationary metabolic flux analysis. *Journal of Experimental Botany* 72: 6087–6090.
- Wieloch T, Ehlers I, Yu J, Frank D, Grabner M, Gessler A, Schleucher J. 2018. Intramolecular ¹³C analysis of tree rings provides multiple plant ecophysiology signals covering decades. *Scientific Reports* 8: 5048.
- Wieloch T, Grabner M, Augusti A, Serk H, Ehlers I, Yu J, Schleucher J. 2022. Metabolism is a major driver of hydrogen isotope fractionation recorded in tree-ring glucose of *Pinus nigra*. *New Phytologist*.
- Wilhelm C, Selmar D. 2011. Energy dissipation is an essential mechanism to sustain the viability of plants: the physiological limits of improved photosynthesis. *Journal of Plant Physiology* 168: 79–87.
- Xu Y, Fu X, Sharkey TD, Shachar-Hill Y, Walker BJ. 2021. The metabolic origins of non-photorespiratory CO₂ release during photosynthesis: a metabolic flux analysis. *Plant Physiology* 186: 297–314.

Supporting Information

Additional Supporting Information may be found online in the Supporting Information section at the end of the article.

Notes S1 Leaf gas exchange measurements.

Notes S2 Estimation of intercellular CO₂ concentrations during growth chamber experiments.

Notes S3 Dilution of isotope signals by remnant starch.

Notes S4 Deuterium fractionation by glucose-6-phosphate dehydrogenase.

Notes S5 Deuterium fractionation by phosphoglucose isomerase.

Please note: Wiley Blackwell are not responsible for the content or functionality of any Supporting Information supplied by the authors. Any queries (other than missing material) should be directed to the *New Phytologist* Central Office.